Preferential adsorption to air-water interfaces: a novel cryoprotective mechanism for LEA proteins

Fanny Yuen[1a], Matthew Watson[1b], Robert Barker[2c], Isabelle Grillo[2], Richard K. Heenan[3], Alan Tunnacliffe[1] and Alexander F. Routh[1‡]

[1]Dept. of Chemical Engineering and Biotechnology, University of Cambridge, Philippa Fawcett Drive, Cambridge CB3 0AS, United Kingdom

[2]Institut Laue Langevin, Grenoble, Cedex 9, France

[3]ISIS Facility, Science & Technology Facilities Council, Rutherford Appleton Laboratory, Chilton, Oxon OX11 0QX, United Kingdom

a. Current address: Proctor and Gamble, Temselaan 100, Grimbergen, 1853, Belgium

b. Dept of Biochemistry, Tennis Court Road, Cambridge

c. University of Kent

[‡]To whom correspondence should be addressed. E-mail: afr10@cam.ac.uk

Abstract

Late embryogenesis abundant (LEA) proteins comprise a diverse family whose members play a key role in abiotic stress tolerance. As intrinsically disordered proteins, LEA proteins are highly hydrophilic and inherently stress tolerant. They have been shown to stabilize multiple client proteins under a variety of stresses, but current hypotheses do not fully explain how such broad range stabilization is achieved. Here, using neutron reflection and surface tension experiments, we examine in detail the mechanism by which model LEA proteins, AavLEA1 and ERD10, protect the enzyme citrate synthase from aggregation during freeze-thaw. We find that a major contributing factor to citrate synthase aggregation is the formation of air bubbles during the freeze-thaw process. This greatly increases the air-water interfacial area, which is known to be detrimental to folded protein stability. Both model LEA proteins preferentially adsorb to this interface and compete with citrate synthase, thereby reducing surface induced aggregation. This novel surface activity provides a general mechanism by which diverse members of the LEA protein family might function to provide aggregation protection that is not specific to the client protein.

Keywords: freeze-thaw; stress tolerance; anhydrobiosis; neutron reflection; protein aggregation

Introduction

Late embryogenesis abundant (LEA) proteins comprise a diverse family of intrinsically disordered proteins (IDPs) that are thought to play a key role in tolerance to abiotic stresses such as freezing and desiccation. These proteins are of particular interest because their link to advancement in stress-tolerant technologies and development in novel biomedical preservation techniques. Originally identified almost 40 years ago in cotton seed embryos LEA genes have since been found in a variety of different organisms, where their presence and expression correlates with the acquisition of stress tolerance (for reviews see (1-3)). LEA proteins are highly variable in sequence, molecular mass and charge and have been classified into twelve different groups (4). However, there is no evidence that members of any particular group carry out distinct functions *in vivo*. As intrinsically disordered proteins (IDPs), LEA proteins are hydrophilic and contain little or no secondary structure. This makes LEA proteins inherently tolerant to conditions that denature folded proteins, and they are thought to stabilise folded cellular proteins under conditions of abiotic stress. Several hypotheses have been proposed regarding the function of LEA proteins in stress tolerance (5-8), but the underlying mechanisms remain unclear.

Interestingly, the protective efficacy of LEA proteins is not specific to the proteins of stress tolerant organisms. For example, Goyal *et al.* (9) showed that AavLEA1, from the anhydrobiotic nematode, *Aphelenchus avenae*, provides anti-aggregation activity for pig heart citrate synthase (CS) and rabbit muscle lactate dehydrogenase under conditions of cold and desiccation stress. Chakrabortee *et al.* (10) demonstrated that AavLEA1 can prevent aggregation of human, as well as nematode, water-soluble proteomes. Furthermore, LEA protein protection is not limited to freeze and desiccation stresses, as AavLEA1 decreased the rate of aggregation of spontaneously aggregating proteins *in vitro* and *in vivo* in the absence of any stress (10, 11). The ability to prevent aggregation, which is not specific to the client protein or the stress, suggests that LEA proteins have a broad protein stabilisation function.

To gain a better understanding of the protective mechanism, we examine in detail a characteristic feature of LEA proteins: their ability to protect model folded proteins from aggregation through repeated cycles of freeze-thaw. We use CS as our model globular protein, and AavLEA1 (12) and ERD10 (13) as our model LEA proteins. Using a combination of pendant drop surface tension measurements and neutron reflection experiments, we find that CS, AavLEA1 and ERD10 are all surface active. However, the LEA proteins adsorb more rapidly to the interface and effectively out-compete CS, thereby reducing surface-induced CS aggregation. This novel LEA protein activity provides a general mechanism whereby members of this diverse family might provide non-specific protection to multiple folded proteins within cells during cold stress. It could also be relevant to other stresses where surface activity is a significant vector for protein denaturation.

Results

AavLEA1 supresses aggregation of CS during freeze-thaw stress

CS is prone to aggregation upon freeze-thaw and has previously been used to examine the protective role of LEA proteins (8-10). We first confirmed that AavLEA1 could suppress CS aggregation during freeze stress in pure water, without the influence of buffer components (14). When subjected to successive rounds of rapid freezing in liquid nitrogen followed by thawing at 20°C, CS samples showed an increase in turbidity (measured by apparent absorbance at 340 nm; A_{340}), which is indicative of light scattering by protein aggregates in suspension (Figure 1a). In contrast, when both CS and AavLEA1 were present in solution at a 1:1 CS:AavLEA1 mass ratio (~1:5 CS:AavLEA1 molar ratio), samples exhibited consistently low turbidity values, similar to those prior to application of the stress.

AavLEA1 alone does not aggregate under these conditions (data not shown). These results are consistent with those reported by Goyal et al. (9).

No LEA protein-client interactions in the bulk either before or after freezing

It has been proposed that the protective effect of LEA proteins involves little, or at most only transient, interaction with client proteins, and they have therefore been termed "molecular shields" (8). However, any such interactions are usually assayed in the absence of stress, and a detailed understanding of any LEA-client interactions or structural changes in either partner that occur upon freeze-thaw is lacking.

In order to examine this we chose to use Small Angle Neutron Scattering (SANS). Because we were able to produce both hydrogenated and deuterated AavLEA1 recombinantly in *Escherichia coli*, we were able to use contrast matching to look at the individual components in the mixture. The contrast of the solvent can be changed by altering the H_2O/D_2O ratio allowing the selective "matching out" of deuterated AavLEA1 with 100% D_2O and hydrogenated CS with 42% D_2O.

Before looking at the CS and AavLEA1 proteins together, it was important to confirm that deuteration of the protein did not adversely affect function, since the strength of hydrogen bonds and the pKa values of ionisable groups in the protein will be different depending on whether H or D is present. Therefore, we compared the ability of hydrogenated AavLEA1 (H-AavLEA1) and deuterated AavLEA1 (D-AavLEA1) proteins to protect CS from freeze-thaw-induced aggregation in both H_2O and D_2O. Furthermore, any effects on secondary structure were assessed by circular dichroism (CD) spectroscopy. As shown in Figures 2d and e, both H-AavLEA1 and D-AavLEA1 proteins provided similar levels of freeze-thaw protection in both solvents, and the CD spectra of both proteins (Figure 3) have very similar shapes, with a large "random-coil" minimum and evidence of a small amount of secondary structure, typical of IDPs.

The SANS pattern from CS dispersed in D_2O is shown in Figure 2a. The data fit well to a prolate ellipsoid model of CS with the two radii being 18.0 ± 0.2 Å and 45.1 ± 0.2 Å. The scattering patterns and fits for the AavLEA1 proteins are shown in Figures 2b and c. It is clear the scattering patterns of the H-AavLEA1 and D-AavLEA1 proteins look different. Intriguingly, while the H-AavLEA1 protein scattering fits to a Gaussian coil with a radius of

gyration of about 33 Å, as one might expect for a disordered protein, the D-AavLEA1 protein does not, and was best fit by a correlation length model of size 13 Å. Presumably this indicates that while both proteins are similar in terms of secondary structure, the overall ensemble of structures populated by the D and H forms are different. A common assumption in neutron scattering is that deuteration does not affect a molecules structure, but this is clearly not the case here; perhaps IDPs are more prone to the subtle differences induced by replacing H with D (15-17). Another possibility is that the high concentrations used for the SANS experiments induced a weak aggregation in the D-LEA and hence the different scattering pattern. However, any structural changes did not appear to significantly affect function, with the H- and D-AavLEA1 proteins both protecting CS from freeze-thaw-induced aggregation in both H_2O and D_2O, (Figures 2d and e). Consequently, we proceeded to examine the individual proteins and the mixtures of CS with H- or D-AavLEA1 both before and after freeze-thaw stress. The scattering profiles of the two proteins in the mixture corresponded to those of the individual proteins, consistent with previous data showing that there is no interaction between AavLEA1 and CS.

Next, samples were subjected to one or three rounds of freeze-thaw and scattering profiles were recorded. Samples containing CS alone were seen to visibly aggregate following freeze-thaw. Consistent with this, SANS curves, (Figure 4a), showed an upturn at low Q which was progressive with successive rounds of freeze-thaw, indicative of aggregation. Interestingly, there were no major changes in the high Q region of the scattering curve, suggesting that any conformational changes in the CS dimer are only minor. In the presence of AavLEA1, this upturn was not observed (Figure 4b) and the curves for different numbers of freeze-thaw cycles overlay. Additionally, the profiles for AavLEA1 look identical to those observed before freeze-thaw. Taken together, these data show that there is no apparent change in protein structure or long-range ordering of the system, even after three cycles of freeze-thaw. It is important to note that we have not measured the system in the frozen state, so we are unable to rule out the involvement of transient interactions that occur during freezing and thawing, our data indicate that any interactions do not endure beyond the imposition of stress.

How the air-liquid interface is created can affect protein aggregation

During the freeze-thaw process, a large number of air bubbles were observed. Protein denaturation and/or aggregation at interfaces is a well-known phenomenon (18-21).

Therefore, we investigated the effect of bubble formation on CS stability using several complementary methods.

First, the concentration of dissolved gasses was reduced by vacuum degassing samples prior to each freezing cycle. The degassed CS samples, even without the addition of AavLEA1, showed reduced turbidity (Figure 1a), confirming that dissolved gasses were, at least in part, responsible for CS aggregation during freeze stress. However, degassing samples did not reduce CS aggregation to the levels observed in the presence of AavLEA1. This difference might be due to incomplete degassing or to the effect of other interfaces or stressors.

Another factor that influences bubble formation is freezing rate. Dissolved gasses are excluded from ice crystals during the freezing process. Rapid freezing traps the bubbles, which remain in the sample until thawing occurs. In contrast, at low freezing rates, these gas bubbles have time to coalesce, reducing the surface area, and are pushed in front of the ice surface, allowing them to escape as the sample freezes (22). Freezing rate also influences the surface area of the ice-water interface produced. Hence, slower freezing is less detrimental to protein stability (23, 24). Consistent with this, CS samples flash frozen in liquid nitrogen gave much higher turbidity readings than identical samples frozen at -80°C or -20°C, with the latter showing very little evidence of aggregation (Figure 1b).

Finally, we investigated the effect on CS aggregation of bubble formation in the absence of freeze-thaw stress; this was achieved by sonication, which induces cavitation (the formation and collapse of tiny bubbles within a liquid due to rapid and intense pressure changes) in the sample (Figure 1c). Ultrasonic treatment is known to cause protein condensation at the surface of gas bubbles, forming aggregates (25). Samples of CS in the absence or presence of AavLEA1 were subjected to multiple rounds of sonication using an ultrasonic probe and aggregation was monitored as before. CS alone readily aggregated; turbidity readings were much higher than observed during freeze-thaw assays, indicating that either more of the protein had aggregated or that larger aggregates had formed. Interestingly, samples containing CS and AavLEA1 showed much lower levels of aggregation after cavitation, significant measurable aggregation not seen until after three rounds of cavitation, suggesting that the mechanism of protection by AavLEA1 involves gas-liquid interfaces. In contrast to the freeze-thaw experiments, protection was incomplete. This may be due to the heating that occurs during sonication, as AavLEA1 alone cannot prevent thermal aggregation of CS (9).

Air-liquid interfaces are characteristic of both flash freezing and sonication; therefore, we hypothesised that the mechanism of protection by LEA proteins during freeze-thaw may be related to the propensity of air-water interfaces to promote protein aggregation. We note that such a mechanism would be independent of LEA-client protein interactions.

LEA proteins adsorb to air-water interfaces in preference to CS

The foamability and foam stability of a protein solution are dependent on adsorption rates and the structure of proteins at the interface. Good foamability correlates with a protein's affinity for the air-water interface, which results in increased adsorption and a more rapid decrease in dynamic surface tension.

The foaming properties of CS and AavLEA1 were found to be very different. Foamability of CS samples was very low; when shaken, CS samples formed a few bubbles which immediately collapsed, and the foam height was considered negligible. In contrast, AavLEA1 solutions formed foams that were stable for several hours. This difference in foamability indicates that AavLEA1 adsorbs to the air-water interface more readily than CS. Figure 5 shows the foam collapse profile of CS, AavLEA1 and a mixture of CS and AavLEA1. While CS showed negligible foaming, both AavLEA1 and the mixture of the two proteins showed similar foam collapse profiles, indicating that the foaming properties of the mixture are dominated by the disordered LEA protein.

To examine the adsorption at the air-water interface over time, dynamic surface tension profiles for CS, AavLEA1 and mixtures of the two proteins were measured using the pendant drop method (Figure 6a). Briefly, the protein concentration at a newly created interface is zero; therefore, the surface tension when a surface is created is expected to be that of pure water. Surface tension then decreases as protein adsorbs to the interface, until the interface is saturated. The profile for AavLEA1 resembles that of a typical surfactant; surface tension rapidly decreased until around 60 s and then plateaued, indicating that equilibrium had been reached. Interpretation of the CS data is more complicated. There is an initial decrease in surface tension over the first 150-200 s, and then a second (slower), decrease that does not reach completion even after 900 s. Presumably, the first process represents adsorption of native CS to the interface, and the second slower process represents a structural rearrangement or denaturation of the globular protein at the interface, because exposure of hydrophobic residues would lower the surface energy.

The initial decrease in dynamic surface tension for AavLEA1 was more rapid than for CS, indicating that AavLEA1 became established at the interface more quickly. This is consistent with our foaming results.

Adding increasing concentrations of AavLEA1 to CS resulted in the dynamic surface tension profiles of the mixtures converging with that of AavLEA1 alone. At low AavLEA1 concentrations, the mixture still exhibited an initial "fast" decrease in surface tension, similar to AavLEA1, but then a second much slower decrease, similar to CS, indicating that some CS reaches the interface. When sufficient AavLEA1 was present, the profiles looked almost identical to that of AavLEA1 alone, suggesting that CS did not populate the surface significantly. This is similar to observations made for protein/surfactant mixtures, where the surfactant out-competes the protein to dominate the interface (26, 27). Taken together, the surface tension data suggest that AavLEA1 adsorbs to the surface more quickly than CS, and in the presence of sufficient AavLEA1, CS competes poorly for access to the surface.

The foaming and surface tension data, taken together, are consistent with the observation that proteins with more flexible structures tend to bring about more rapid changes in dynamic surface tension and form more stable foams than those with rigid structures [29-31].

To demonstrate that the competitive adsorption effect was not limited to AavLEA1, similar freeze-thaw and surface tension experiments were performed with another LEA protein, ERD10, from *Arabidopsis thaliana*. Despite significantly different characteristic amino acid signatures, and being from a different LEA protein group, freeze-thaw experiments showed that ERD10 also provided good protection against CS aggregation (Figure 1d). Dynamic surface tension experiments showed that like AavLEA1, ERD10 also adsorbed at the air-water interface preferentially to CS (Figure 6b).

Neutron reflection analysis of the surface layer conformations of LEA and globular proteins at air-water interfaces

The dynamic surface tension data provided evidence that AavLEA1 preferentially adsorbs to the air-water interface; however, the method was unable to easily differentiate the contributions of each protein in the mixtures. Therefore, to provide a fuller picture of the system, neutron reflection was used. Deuterated AavLEA1 protein was grown recombinantly as described in the Materials section. This allowed different components in the protein mixture to be individually examined. In 100% D_2O, only contributions from the air-water

interface and hydrogenated proteins are detected (deuterated proteins are “matched out”). In 42% D_2O, only contributions from deuterated proteins and the substrate are recorded (hydrogenated proteins are “matched out”). Finally, using “air contrast matched water” (ACMW; 8% D_2O), contributions from the substrate (water) can be “matched out”. By simultaneously fitting the data from multiple different contrasts, density profiles for each protein can be calculated.

The standard layer approaches customarily used to fit neutron reflection data were insufficient to accurately describe our system. Therefore, a new custom layer model approach was used. This layer model contains thickness as a fitted variable and assumes that there is no protein at either the top (i.e. the air boundary) or at the bottom of the layer. This surface layer was split into four or five slabs of equal thickness. Within each slab, the protein contribution could be fitted at the midpoint and the data in-between these points was constructed using PCHIP interpolation. In systems containing more than one protein, the summated total curve was deconvoluted to give the contributions of the individual proteins. The raw data and the corresponding fits are shown in the insert to the protein density curves.

First, the two proteins were examined individually. The reflectivity profiles of CS in water after equilibrating for 2 h, in three different water contrasts, are shown in the insert to Figure 7a. The fit to the data is shown as solid lines, resulting in the protein density profile shown in Figure 7a. This shows a double layer configuration with a total thickness of around 8 nm. The layer closest to the air-water interface was estimated to be around 2.5 nm thick, which is too small to be native CS, suggesting that the protein at the surface has undergone a structural rearrangement and become denatured after 2 h. This is consistent with our surface tension observations, where we hypothesise that after initial adsorption to the surface, CS then Undergoes a slower conformational rearrangement. The second CS layer had a thickness around 5 nm, which is roughly the diameter of folded CS (28), suggesting that this second layer comprises native protein.

The insert of Figure 7b shows the reflectivity profiles for both hydrogenated-AavLEA1 (H-AavLEA1) and deuterated-AavLEA1 (D-AavLEA1) proteins in three different water contrasts after 2 h. These profiles are simultaneously fit to provide the protein density profile shown in Figure 7b. In contrast to the CS result, AavLEA1 formed a concentrated layer approximately 2 nm thick at the interface, with a more diffuse zone extending to a depth of 5 nm below the interface. It is difficult to draw detailed conclusions about the structure of

AavLEA1 at the interface because the protein is intrinsically disordered; however, the thickness of the dense layer closest to the surface is smaller than the size of a single AavLEA1 molecule, determined by SANS as 3.3 nm. This suggests that the AavLEA1 protein takes a conformation at the interface which is more compact than in the bulk. The simultaneous fit of H and D AavLEA1 indicates that the proteins take up similar structures as the air-water interface. This contradicts the finding in Figure 2 b and c, showing a difference in bulk structure. Hence our belief that the difference only occurs in the bulk at elevated concentrations. Previous Fourier transform-infrared studies have shown that AavLEA1, although natively unfolded in bulk solution, could be induced into helical formations by drying (29), consistent with computer modelling if the AavLEA1 and other similar LEA protein structures (29, 30). Similar to drying, the air-water interface also decreases protein hydration and exerts a thermodynamic pressure for AavLEA1 to adopt a more compact structure. These neutron reflection results confirm that both AavLEA1 and CS have the propensity to adsorb to the air-water interface, which is consistent with the surface tension measurements.

Next, competitive adsorption experiments using mixtures of CS and AavLEA1 were conducted at a single detector position over 30 s intervals. This allowed data to be collected at short time points showing how the protein density profiles evolve with time (Figure 8). All contrasts were fit simultaneously and, in all profiles, the surface was clearly dominated by AavLEA1. Consistent with the dynamic surface tension measurements, a significant amount of AavLEA1 had adsorbed to the surface after only 30 s, forming two distinct layers. No contribution from CS was apparent until the 30-min time point, when a small amount of CS was detected around 5 nm below the interface. By 60 min, some CS started to appear in a bilayer conformation. By 2 h, a measurable bilayer of CS was formed at the interface; however, the layer of protein closest to the interface was still predominantly composed of AavLEA1. These results provide further evidence that AavLEA1 outcompetes CS for access to the interface over short time frames, and thus reduces surface-induced aggregation of CS.

Discussion

Proteins have been shown to lose biological activity after exposure to interfaces (31, 32). In solution, globular proteins are marginally stable (33) and their adsorption to interfaces causes aggregation (18, 19). During the freeze-thaw process many new interfaces are created, most notably those associated with air bubbles, due to the precipitation of dissolved gasses during

freezing, and ice crystals. Proteins readily adsorb to these interfaces, which are believed to be denaturation sites for folded proteins (23, 34-37). Here, we investigated two IDPs associated with tolerance to water stress, the LEA proteins AavLEA1 and ERD10, which protect a model globular protein, CS, from freeze-thaw-induced protein aggregation. In comparison to globular proteins, LEA proteins are usually lower in molecular mass and far more flexible in structure. Although they contain a high proportion of charged and polar amino acids, LEA proteins also contain hydrophobic residues, and both types of residue are potentially available for interaction with interfaces. Our results provide evidence that AavLEA1 outcompetes CS at an air-water interface, and that this ability may allow AavLEA1 to protect CS from surface-induced denaturation. These findings have led us to propose preferential adsorption to interfaces as an additional, novel mechanism by which LEA proteins can stabilise folded proteins during stress. We hypothesize that this activity, during freeze-thaw, effectively restricts a protein such as CS to the bulk liquid, thus protecting it from denaturation at the interface (Figure 9). This new mechanism is consistent with studies showing that the aggregation of proteins exposed to air-water interfaces can be reduced by the addition of surfactants (20, 23). LEA proteins could fulfil a similar role to that of the surfactants in these studies, but with the advantage of better biological compatibility. In this study, we have mainly focused on the effect of air-water interfaces; however, the effect of solid ice interfaces should not be dismissed (23, 34-37), particularly since our degassing experiments suggest that additional factors contribute to CS denaturation upon freeze-thawing.

The proposal that LEA proteins adsorb to interfaces as a method of globular protein protection aligns with the evidence that protection is non-specific with respect to client protein, LEA protein, and the type of stress. LEA proteins protect a variety of different folded proteins and even entire proteomes from desiccation-induced aggregation (9, 10). In addition, there are many LEA proteins, with varying amino acid motifs, which have been shown to protect against freeze stress (38-40). The group 2 (ERD10) and group 3 (AavLEA1) LEA proteins used in this study were both shown to provide good protection for the same client protein, even though their sequences, molecular mass and signature motifs significantly differ. An interfacial adsorption mechanism would only require the LEA protein to out-compete the client protein for the interface. As unstructured, low molecular weight macromolecules, these characteristics would be expected for any LEA protein with the correct hydrophilic-hydrophobic balance.

The proposed preferential adsorption model for LEA proteins provides a general mechanism that explains how LEA proteins are able to protect client proteins from aggregation under a variety of stresses. However, even in the absence of any stress, interfaces can be damaging to proteins. LEA proteins have been shown to decrease the rate of aggregation of spontaneously aggregating polyQ proteins *in vitro* and *in vivo* (10, 11). Recent observations suggest that polyQ proteins may have the propensity to aggregate at gas bubble interfaces (41). Therefore, interfacial adsorption of LEA proteins may also play a significant role in preventing polyQ aggregation. Since interfacial competition by LEA proteins is a general aggregation protection mechanism (i.e. one that does not require specific interaction with a client protein), the results from this work may be applicable to other protein systems where interfaces are found to nucleate protein aggregation, e.g. amyloids characteristic of Alzheimer's disease (42).

The tendency of LEA proteins to migrate to air-water interfaces is reminiscent of models that explain their protection of lipid bilayers under water-stress conditions. Thus, various LEA proteins are thought, during cold stress or dehydration, to fold into amphipathic helices that become embedded laterally in the surface of the membrane (43, 44). In this 'snorkeling' model (45, 46), the hydrophobic surface of the helix penetrates below the headgroup region of the bilayer to interact with the fatty acid side chains of the phospholipids (44, 47). The hydrophilic face of the LEA protein remains in contact with the headgroups and any associated water molecules. The air-water interface in gas bubbles might also provoke folding of LEA proteins into helices such that the hydrophobic face projects into air, while the hydrophilic surface remains in the liquid phase.

The neutron reflectivity and surface tension data suggest that both CS and AavLEA1 rearrange upon contact with the air-water interface. CS adsorption sees a two stage reduction in surface tension which we ascribe to adsorption and then a subsequent slower rearrangement. This is consistent with the neutron reflectivity data, which shows a surface layer smaller than the native bulk CS. Adsorption of AavLEA1 has only a single relaxation time in the surface tension measurements, indicating that any rearrangement does not correlate with a surface tension reduction. The neutron reflection data shows a surface layer which is more compact than the native protein, again indicating a change in structure. We note also that the IDP can be easily redispersed and does not denature, showing that any surface induced structure is transitory. Our comments about interface induced restructuring

are indirect conjectures from the surface tension and reflectivity. It would be desirable to obtain a direct measure of structure at the interface and this is the subject of future work.

The preferential adsorption of LEA proteins to the air-water interface is also, to some extent, comparable with the Vroman effect, which describes the competitive adsorption of proteins to a solid surface (48). In a mixture of proteins, smaller or more highly concentrated proteins are the first to arrive at and adsorb to a solid-liquid interface, and these are later displaced by proteins of higher molecular mass (49). Similarly, for mixtures of CS and LEA protein, our neutron reflection data suggest that, although initially AavLEA1 dominates the air-water interface, CS can begin to compete for the surface over long time periods. Whether such an exchange would occur at an appreciable rate at low temperatures is perhaps unlikely, particular where cells freeze.

IDPs are known to protect globular proteins through both freeze-thaw and dessication stresses. In this work we have only examined the freeze-thaw induced aggregation although we note that the presence of air-water interfaces is common to the stresses that IDPs are known to offer protection from.

Taken together our results indicate that AavLEA1 effectively competes with CS for access to the interface over short time-scales, providing protection against surface-induced aggregation in freeze-thaw assays. However, the data from longer time points indicate that CS does eventually accumulate at the interface. We speculate that while AavLEA1 competes well with the initial association of native CS with the surface, some CS is still able to adsorb and denature. Once denatured, CS cannot be efficiently displaced by AavLEA1, due to higher surface activity of the denatured protein. Nor can the LEA protein act as a chaperone to sequester or aid refolding. Therefore, LEA proteins act as kinetic stabilisers, providing effective protection during short periods of stress, but over long periods are less effective.

The role of IDPs in stress tolerance continues to be an important area of scientific research. In this study, we have demonstrated that some IDPs have surface activity and propose this as a mechanism by which they prevent the aggregation of sensitive globular proteins during the freeze-thaw process. These novel findings enhance our understanding of the biophysical and biochemical properties of IDPs in relation to their involvement in stress tolerance and may be of value in the development of novel biopreservation techniques.

Materials and Methods

Proteins

Pig heart citrate synthase was purchased from Sigma Aldrich as an ammonium sulphate suspension, and dialysed into water immediately prior to use.

Recombinant AavLEA1 was expressed in *E. coli* BL21(DE3) cells, transformed with pET15b containing the AavLEA1 gene with an N-terminal thrombin cleavable hexa-histidine tag as described previously (29) with the modification that after induction with isopropyl-β-D-thiogalactopyranoside (IPTG), cultures were grown at 23ºC for a further 12 h. Cells were harvested by centrifugation, washed by resuspending in 10 mM Tris pH 7.4 and 100 mM NaCl, recentrifuged and pellets stored at -20ºC. Cells were later thawed and resuspended in IMAC A (10 mM sodium phosphate pH 8.0, 0.5 M NaCl and 10 mM imidazole) with "complete" EDTA-free protease inhibitor cocktail (Roche) before lysis by sonication. After sonication, the lysate was clarified by centrifugation at 18,000 rpm for 20 min, and the supernatant was heated to 100ºC for 20 minutes before being recentrifuged at 13,000 rpm for 10 min. The supernatant was passed through a 0.22 µm PVDF syringe filter and applied to a nickel chelation column (His-catch, Bioline or HisTrap FF Crude, GE Healthcare) pre-equilibrated with IMAC A. Bound proteins were eluted with IMAC B (10 mM sodium phosphate pH 8.0, 0.5 M NaCl and 400 mM imidazole). The histidine tag was removed by cleavage with thrombin, which was subsequently removed by passing over *p*-aminobenzamidine agarose (Sigma Aldrich). Samples were extensively dialysed against water and concentrated using an Eppendorf 5301 vacuum concentrator in a cold room. AavLEA1 concentration was determined by absorbance at 280 nm using a molecular mass of 16,309.66 g/mol and a molar extinction coefficient of 8,250 M^{-1} cm^{-1}.

Deuterated AavLEA1 was expressed and purified as described for AavLEA1 with the following modifications. After transformation, cells were acclimatised by plating sequentially onto LB agar plates containing 20%, 40%, 60% and 80% D_2O. All growth steps were subsequently carried out in M9 minimal medium containing 100% D2O. After induction with IPTG, cultures were grown at 23ºC for a further 48 h. Deuterium incorporation was determined by mass spectrometory (Protein & Nucleic Acid Chemistry Facility, Department of Biochemistry University of Cambridge) and found to be ~90% for non-exchangeable protons.

The coding sequence for *A. thaliana* ERD10 (European Nucleotide Archive EMBL-CDS: D17714.1) was PCR amplified from a plasmid (50) provided by David Macherel (University

of Angers, France) and inserted into pHAT3.1 (based on pHAT3 (51) but with a modified polylinker in which the second BamH1 site has been removed) which contains an N-terminal thrombin cleavable hexa-histidine tag, using BamHI and EcoRI. Recombinant ERD10 was expressed and purified essentially as described for AavLEA1. However, after removal of the histidine tag ERD10 was dialysed into 20 mM Tris pH8.0 before further purifying on a 6 mL Resource Q column (GE Healthcare) using a linear salt gradient from 0-1M NaCl over 100 mL. The purified protein was then dialysed extensively against H_2O, and the concentration determined by absorbance at 280 nm using a molecular mass of 29,691.90 g/mol and a molar extinction coefficient of 2560 M^{-1} cm^{-1}.

***In vitro* protein freeze-stress aggregation assay**

Samples of 200 µL were loaded into a 96-well plate, submerged in liquid nitrogen for 10 min, and thawed at 20°C. After each freeze-thaw cycle, the extent of aggregation was determined by measuring the apparent absorbance at 340 nm using a Wallac EnVision 2104 Multilabel plate reader. To examine the effect of degassing, samples were degassed for 10 min in an Eppendorf 5301 vacuum concentrator in advance of each freeze-thaw cycle. Different freezing rates were achieved by substituting the liquid nitrogen freezing step with placing the samples in a -20°C freezer or -80°C freezer for 8 h.

Cavitation-stress aggregation assay

Cavitation was induced in 400 µl samples using an ultrasonic probe; SLPe Digital Sonifier (Branson™) in a cold room. Cycles were 30 minutes at 10% amplitude. After each cycle aggregation was measured by apparent absorbance at 340 nm using a Wallac EnVision 2104 Multilabel plate reader.

Foaming performance

The Bartsch cylinder shake test (52) was used to evaluate the foaming collapse profiles of protein solutions. Closed 10 mL cylinders with 1 mL each protein solution were vigorously shaken by hand 10 times, once per second, over 10 s. The foam volume was measured at various time points over 6.5 h. The foamability of a solution was characterised by the foam volume immediately after shaking, and the foam stability was characterised by the foam volume remaining after a certain period.

Surface tension measurements

Surface tension data was obtained using a DSA 100 Drop Shape Analysis System (Krüss GmbH, Germany). Approximately 25 µL drops of protein in water at various concentrations were suspended from a 1.830 mm diameter syringe needle. Photos were taken at an average speed of 3 fps and the drop shape was monitored over 15 min. The shape factor was iterated from the photos of the drops by the DSA1 software. Times shown in the data denote the time since the first measurement. It takes approximately eight seconds, from the first depression of the syringe plunger (liquid exiting the needle), for the drop to be formed and to stabilize. Therefore, changes during the first eight seconds are not measured using this system.

SANS measurements

Small angle neutron scattering experiments were performed with the Sans2D time-of-flight instrument at ISIS located at the Rutherford Appleton Laboratory in Oxfordshire, UK. The detector length was 4 m and the incident wavelength of the neutron beam was 1.75 – 16.5 A. This gave a Q range of 0.005 to 0.6 A^{-1}. QS quartz banjo cells with an optical path of 0.5 or 1 mm were used. Temperature control was carried out using 5 kW circulating fluid baths and set to 7°C. Typically, data were collected for 30 min and then corrected and normalised to an absolute scale by background subtraction. Data were analysed using the SASview-2.2.1 program (www.sasview.org).

The freeze-thaw experiments were performed using 0.25 or 0.5 mL samples contained in 1.5 mL Eppendorf tubes. The samples were frozen for 5 min in liquid nitrogen and thawed in an ambient temperature water bath for 7 min. Three models were used to fit the SANS data. For CS an ellipsoid model describing an ellipsoidal particle with a uniform scattering length density and without inter-particle interactions was used. For H-AavLEA1, a polydisperse Gaussian-coil model was used. This describes polymer chains with a well-defined molecular weight distribution. For D-AavLEA1 a correlation length model was used. This is an empirical model which describes the representative length scale for the protein chains.

Neutron reflection at air-water interface

Neutron reflection experiments were undertaken on the Fluid Interfaces Grazing Angles ReflectOmeter (FIGARO) time-of-flight reflectometer at the Institut Laue-Langevin (ILL), Grenoble, France. The protein solutions were loaded onto low-volume delrin troughs with a positive meniscus to ensure that the trough itself does not obstruct the incoming or reflected

neutron beams. The troughs were mounted onto an active antivibration table and automatically aligned using a high precision optical sensor. The temperature was set at 20°C.

Measurements were conducted at one incident angle and at a wavelength range of 2 Å < λ < 30 Å, which covers a *Q*-range from 0.008 to 0.4 $Å^{-1}$. All noted surface ages are measured from the time of sample spreading. For single protein samples and for the CS + AavLEA1 sample measured at 2 h, the measurement time ranged from 45 min to 1.5 h, depending on the contrast. For younger surface ages, the data was collected for 30 s.

The reflectivity profiles were fit to provide protein concentration versus depth profiles. The fitting procedure involved binning the protein concentration into five layers with a fixed concentration in each layer and fitting all contrasts simultaneously. The reflectivity profiles and fitting procedure are shown in the insert to each protein density curve.

Far-UV CD spectroscopy

CD spectra of H-AavLEA1 and D-AavLEA1 at a concentration of 8-12.3 μM in H_2O, 42% D_2O and D_2O were recorded over the range 190-250 nm using an AVIV 410 spectrometer. Spectra were recorded at 25ºC in a 1 mm path-length cuvette with a data pitch of 1 nm and an averaging time of 2 seconds and baseline corrected against the appropriate solvent before applying smoothing. Measured ellipticity values were converted to mean residue ellipticities (MRE) with units deg cm^2 $dmol^{-1}$ to normalise for differences in concentration.

Acknowledgements

FY thanks the Natural Sciences and Engineering Research Council of Canada for a PhD scholarship. AT was supported by a European Research Council Advanced Investigator Grant 233232. The authors are grateful to the Rutherford lab and the Institut Laue Langevin for the granting of beamtime. The ILL data may be found at http://doi.ill.fr/10.5291/ILL-DATA.9-13-540.

The authors declare that they have no conflicts of interest with the contents of this article.

References

1 Tunnacliffe, A., Hincha, D. K., Leprince, O. and Macherel, D. (2010) LEA Proteins: Versatility of Form and Function. In Dormancy and Resistance in Harsh Environments (Lubzens, E., Cerda, J. and Clark, M., eds.). pp. 91-108, Springer Berlin Heidelberg, Berlin, Heidelberg

2 Hand, S. C., Menze, M. A., Toner, M., Boswell, L. and Moore, D. (2011) LEA proteins during water stress: not just for plants anymore. Annu. Rev. Physiol. **73**, 115-134

3 Battaglia, M., Olvera-Carrillo, Y., Garciarrubio, A., Campos, F. and Covarrubias, A. A. (2008) The Enigmatic LEA Proteins and Other Hydrophilins. Plant Physiol. **148**, 6-24

4 Jaspard, E., Macherel, D. and Hunault, G. (2012) Computational and Statistical Analyses of Amino Acid Usage and Physico-Chemical Properties of the Twelve Late Embryogenesis Abundant Protein Classes. PLoS One. **7**, e36968

5 Bokor, M., Csizmok, V., Kovacs, D., Banki, P., Friedrich, P., Tompa, P. and Tompa, K. (2005) NMR relaxation studies on the hydrate layer of intrinsically unstructured proteins. Biophys. J. **88**, 2030-2037

6 Alsheikh, M. K., Heyen, B. J. and Randall, S. K. (2003) Ion binding properties of the dehydrin ERD14 are dependent upon phosphorylation. J. Biol. Chem. **278**, 40882-40889

7 Koag, M. C., Fenton, R. D., Wilkens, S. and Close, T. J. (2003) The binding of maize DHN1 to lipid vesicles. Gain of structure and lipid specificity. Plant Physiol. **131**, 309-316

8 Chakrabortee, S., Tripathi, R., Watson, M., Schierle, G. S. K., Kurniawan, D. P., Kaminski, C. F., Wise, M. J. and Tunnacliffe, A. (2012) Intrinsically disordered proteins as molecular shields. Molecular Biosystems. **8**, 210-219

9 Goyal, K., Walton, Laura J. and Tunnacliffe, A. (2005) LEA proteins prevent protein aggregation due to water stress. Biochem. J. **388**, 151-157

10 Chakrabortee, S., Boschetti, C., Walton, L. J., Sarkar, S., Rubinsztein, D. C. and Tunnacliffe, A. (2007) Hydrophilic protein associated with desiccation tolerance exhibits broad protein stabilization function. Proceedings of the National Academy of Sciences. **104**, 18073-18078

11 Liu, Y., Chakrabortee, S., Li, R., Zheng, Y. and Tunnacliffe, A. (2011) Both plant and animal LEA proteins act as kinetic stabilisers of polyglutamine-dependent protein aggregation. FEBS Lett. **585**, 630-634

12 Browne, J., Tunnacliffe, A. and Burnell, A. (2002) Anhydrobiosis - Plant desiccation gene found in a nematode. Nature. **416**, 38-38

13 Kiyosue, T., Yamaguchi-Shinozaki, K. and Shinozaki, K. (1994) Characterization of two cDNAs (ERD10 and ERD14) corresponding to genes that respond rapidly to dehydration stress in Arabidopsis thaliana. Plant Cell Physiol. **35**, 225-231

14 Kolhe, P., Amend, E. and K. Singh, S. (2010) Impact of freezing on pH of buffered solutions and consequences for monoclonal antibody aggregation. Biotechnol. Prog. **26**, 727-733
15 Fisher, S. J. and Helliwell, J. R. (2008) An investigation into structural changes due to deuteration. Acta Crystallogr. Sect. A: Found. Crystallogr. **64**, 359-367
16 Dennison, S. R., Hauβ, T., Dante, S., Brandenburg, K., Harris, F. and Phoenix, D. A. (2006) Deuteration can affect the conformational behaviour of amphiphilic α-helical structures. Biophys. Chem. **119**, 115-120
17 Chen, C.-H., Liu, I. W., MacColl, R. and Berns, D. S. (1983) Differences in structure and stability between normal and deuterated proteins (phycocyanin). Biopolymers. **22**, 1223-1233
18 Cecil, R. and Louis, C. F. (1970) Protein-hydrocarbon interactions. Interactions of various proteins with decane in the presence of alcohols. Biochem. J. **117**, 147-156
19 Macritchie, F. (1978) Proteins at Interfaces. In Adv. Protein Chem. (C.B. Anfinsen, J. T. E. and Frederic, M. R., eds.). pp. 283-326, Academic Press
20 Maa, Y.-F. and Hsu, C. C. (1997) Protein denaturation by combined effect of shear and air-liquid interface. Biotechnol. Bioeng. **54**, 503-512
21 Wiesbauer, J., Prassl, R. and Nidetzky, B. (2013) Renewal of the Air–Water Interface as a Critical System Parameter of Protein Stability: Aggregation of the Human Growth Hormone and Its Prevention by Surface-Active Compounds. Langmuir. **29**, 15240-15250
22 Carte, A. E. (1961) Air Bubbles in Ice. Proceedings of the Physical Society. **77**, 757
23 Kerwin, B. A., Heller, M. C., Levin, S. H. and Randolph, T. W. (1998) Effects of tween 80 and sucrose on acute short-term stability and long-term storage at −20 °C of a recombinant hemoglobin. J. Pharm. Sci. **87**, 1062-1068
24 Cao, E., Chen, Y., Cui, Z. and Foster, P. R. (2003) Effect of freezing and thawing rates on denaturation of proteins in aqueous solutions. Biotechnol. Bioeng. **82**, 684-690
25 Wu, H. and Liu, S.-c. (1931) Coagulation of egg albumin by supersonic waves. Proc. Soc. Exp. Biol. Med. **28**, 782-784
26 Miller, K. E., Skogerboe, K. J. and Synovec, R. E. (1999) Novel calibration of a dynamic surface tension detector: flow injection analysis of kinetically-hindered surface active analytes. Talanta. **50**, 1045-1056
27 Krägel, J., Wüstneck, R., Husband, F., Wilde, P. J., Makievski, A. V., Grigoriev, D. O. and Li, J. B. (1999) Properties of mixed protein/surfactant adsorption layers. Colloids Surf. B. Biointerfaces. **12**, 399-407
28 Durchschlag, H., Zipper, P., Purr, G. and Jaenicke, R. (1996) Comparative studies of structural properties and conformational changes of proteins by analytical ultracentrifugation and other techniques. Colloid. Polym. Sci. **274**, 117-137
29 Goyal, K., Tisi, L., Basran, A., Browne, J., Burnell, A., Zurdo, J. and Tunnacliffe, A. (2003) Transition from natively unfolded to folded state induced by desiccation in an anhydrobiotic nematode protein. J. Biol. Chem. **278**, 12977-12984
30 Dure, L. (1993) A repeating 11-mer amino acid motif and plant desiccation. Plant J. **3**, 363-369
31 Augenstine, L. G. and Ray, B. R. (1957) Trypsin Monolayers at the Air–Water Interface. III. Structural Postulates on Inactivation. The Journal of Physical Chemistry. **61**, 1385-1388
32 Donaldson, T. L., Boonstra, E. F. and Hammond, J. M. (1980) Kinetics of protein denaturation at gas—liquid interfaces. J. Colloid Interface Sci. **74**, 441-450
33 Dill, K. A. (1990) Dominant forces in protein folding. Biochemistry. **29**, 7133-7155
34 Rey, L. (2010) Freeze-Drying/Lyophilization of Pharmaceutical and Biological Products, Third Edition. CRC Press
35 Schwegman, J. J., Carpenter, J. F. and Nail, S. L. (2009) Evidence of partial unfolding of proteins at the ice/freeze-concentrate interface by infrared microscopy. J. Pharm. Sci. **98**, 3239-3246

36 Krielgaard, L., Jones, L. S., Randolph, T. W., Frokjaer, S., Flink, J. M., Manning, M. C. and Carpenter, J. F. (1998) Effect of tween 20 on freeze-thawing- and agitation-induced aggregation of recombinant human factor XIII. J. Pharm. Sci. **87**, 1593-1603
37 Cordes, A. A., Carpenter, J. F. and Randolph, T. W. (2012) Accelerated stability studies of abatacept formulations: Comparison of freeze–thawing- and agitation-induced stresses. J. Pharm. Sci. **101**, 2307-2315
38 Sasaki, K., Christov, N. K., Tsuda, S. and Imai, R. (2013) Identification of a Novel LEA Protein Involved in Freezing Tolerance in Wheat. Plant Cell Physiol.
39 Hanin, M., Brini, F., Ebel, C., Toda, Y., Takeda, S. and Masmoudi, K. (2011) Plant dehydrins and stress tolerance: Versatile proteins for complex mechanisms. Plant Signaling & Behavior. **6**, 1503-1509
40 Honjoh, K.-i., Matsumoto, H., Shimizu, H., Ooyama, K., Tanaka, K., Oda, Y., Takata, R., Joh, T., Suga, K., Miyamoto, T., Iio, M. and Hatano, S. (2000) Cryoprotective Activities of Group 3 Late Embryogenesis Abundant Proteins from *Chlorella vulgaris* C-27. Biosci., Biotechnol., Biochem. **64**, 1656-1663
41 Akram, M. S. (2013) Functionalised self-assembling polyglutamine fusion tags. In Department of Chemical Engineering and Biochemistry ed.), University of Cambridge, Cambridge, UK
42 Lee, C. F., Bird, S., Shaw, M., Jean, L. and Vaux, D. J. (2012) Combined Effects of Agitation, Macromolecular Crowding, and Interfaces on Amyloidogenesis. J. Biol. Chem. **287**, 38006-38019
43 Thalhammer, A., Bryant, G., Sulpice, R. and Hincha, D. K. (2014) Disordered Cold Regulated15 Proteins Protect Chloroplast Membranes during Freezing through Binding and Folding, But Do Not Stabilize Chloroplast Enzymes in Vivo. Plant Physiol. **166**, 190-201
44 Tolleter, D., Hincha, D. K. and Macherel, D. (2010) A mitochondrial late embryogenesis abundant protein stabilizes model membranes in the dry state. Biochim. Biophys. Acta. **1798**, 1926-1933
45 Segrest, J. P., Jones, M. K., De Loof, H., Brouillette, C. G., Venkatachalapathi, Y. V. and Anantharamaiah, G. M. (1992) The amphipathic helix in the exchangeable apolipoproteins: a review of secondary structure and function. J. Lipid Res. **33**, 141-166
46 Segrest, J. P., De Loof, H., Dohlman, J. G., Brouillette, C. G. and Anantharamaiah, G. M. (1990) Amphipathic helix motif: Classes and properties. Proteins: Structure, Function, and Bioinformatics. **8**, 103-117
47 Bremer, A., Kent, B., Hauß, T., Thalhammer, A., Yepuri, N. R., Darwish, T. A., Garvey, C. J., Bryant, G. and Hincha, D. K. Intrinsically Disordered Stress Protein COR15A Resides at the Membrane Surface during Dehydration. Biophys. J. **113**, 572-579
48 Vroman, L., Adams, A., Fischer, G. and Munoz, P. (1980) Interaction of high molecular weight kininogen, factor XII, and fibrinogen in plasma at interfaces. Blood. **55**, 156-159
49 Slack, S. M. and Horbett, T. A. (1995) The Vroman Effect. In Proteins at Interfaces II. pp. 112-128, American Chemical Society
50 Candat, A., Paszkiewicz, G., Neveu, M., Gautier, R., Logan, D. C., Avelange-Macherel, M.-H. and Macherel, D. (2014) The Ubiquitous Distribution of Late Embryogenesis Abundant Proteins across Cell Compartments in Arabidopsis Offers Tailored Protection against Abiotic Stress. The Plant Cell. **26**, 3148-3166
51 Peränen, J., Rikkonen, M., Hyvönen, M. and Kääriäinen, L. (1996) T7 Vectors with a Modified T7lacPromoter for Expression of Proteins in Escherichia coli. Anal. Biochem. **236**, 371-373
52 Bartsch, O. (1924) Über Schaumsysteme. Kolloidchemische Beihefte. **20**, 1-49
53 Nicolas, G. and C., P. M. (1997) SWISS-MODEL and the Swiss-Pdb Viewer: An environment for comparative protein modeling. Electrophoresis. **18**, 2714-2723

54 Larson, S. B., Day, J. S., Nguyen, C., Cudney, R. and McPherson, A. (2009) Structure of pig heart citrate synthase at 1.78 Å resolution. Acta Crystallographica Section F: Structural Biology and Crystallization Communications. **65**, 430-434

List of Figures

Figure 1: LEA proteins prevent CS aggregation caused by exposure to gas-liquid interfaces. Apparent absorbance at 340 nm of aqueous solutions of (a) CS, CS + AavLEA1, and degassed CS after multiple freeze-thaw cycles; (b) CS after multiple cycles of freeze-thaw at -20°C, -80°C and in liquid nitrogen; (c) CS in the absence and presence of AavLEA1 after multiple cycles of sonication; and (d) CS in the absence and presence of ERD10 after multiple freeze-thaw cycles. Concentrations of CS, AavLEA1 and ERD10 were 0.25 mg/mL. Individual data points for each replicate are shown.

Figure 2: Characterisation of hydrogenated and deuterated AavLEA1 and CS protein. (a) The SANS pattern from 2.5 mg/ml H-CS in D_2O fits an oblate ellipsoid model with two dimensions 18.0 and 45.1 Å (b) The SANS pattern from 2.5 mg/ml H-AavLEA1 in D_2O fits well to a Gaussian coil with radius of gyration 33 Å. The low Q points were removed because of over subtraction of background. (c) The SANS pattern from 2.5 mg/ml D-AavLEA1 in 42% D_2O fits well to a correlation length model with a correlation length of 13 Å. The error bars in the SANS data correspond to the standard deviation in the neutron flux intensity. (d) Freeze-thaw cycle assays for CS and CS + H-AavLEA1 and CS+ D-AavLEA1 in H_2O. (e) Freeze-thaw cycle assays for CS and CS + H-AavLEA1 and CS+ D-AavLEA1 in D_2O.

Figure 3: H-AavLEA1 and D-AavLEA1 are both disordered in solution. Far-UV CD spectra of (a) H AavLEA1 and (b) D-AavLEA1 in H2O, 42% D2O and D2O. Data are displayed as mean residue ellipticities (MRE) to normalise for differences in concentration.

Figure 4: SANS patterns from mixtures of CS and deuterated AavLEA1 after up to three cycles of freeze-thaw. (a) 2.5 mg/ml H-CS in D_2O after zero, one and three cycles of freeze thaw. (b) 2.5 mg/mL H-CS + 2.5 mg/mL D-AavLEA1 mixture in D_2O, after zero, one and three cycles of freeze-thaw. Scattering is only observed from H-CS, and (c) 2.5 mg/mL H-CS + 2.5 mg/mL D-AavLEA1 mixture in 42% D_2O, after zero, one cycle and three cycles of freeze-thaw. Scattering is only observed from D-AavLEA1.

Figure 5: Foam collapse profile of 0.25 mg/mL CS, 0.25 mg/mL AavLEA1 and 0.25 mg/mL CS + 0.25 mg/mL AavLEA1 solutions. Closed 10 mL cylinders with 1 mL of each protein solution were vigorously shaken by hand 10 times, once per second, over 10 s and the foam volume was measured at various time points over 6.5 h.

Figure 6: Dynamic surface tension profiles of 0.6 mg/mL CS, and 0.6 mg/mL CS with various concentrations of LEA proteins (a) AavLEA1 and (b) ERD10. The surface tension of

each solution was monitored over 15 min using the pendant drop method. Time = 0 s denotes the start of measurement at approximately 8 s after the start of drop formation.

Figure 7: Neutron reflectivity profiles for 0.6 mg/ml AavLEA1 protein in water and the resulting depth profile of protein concentration from simultaneous fitting of all reflectivity profiles. (a) 0.6 mg/ml CS in various water contrasts. (b) H- and D-AavLEA1 protein in different water contrasts. In the insert caption D-LEA refers to D-AavLEA1.

Figure 8: Protein concentration profiles as measured by neutron reflection at the air-water interface for 0.6 mg/mL CS + 0.6 mg/mL AavLEA1 in water at various times. (a) 30 s, (b) 1 min, (c) 5 min, (d) 30 min, (e) 60 min, (f) 2 h. The contribution from AavLEA1 is denoted in the blue solid lines, and the CS contribution is shown by the red dotted lines. Inserts to figures show the reflectivity profiles in the various contrasts and the simultaneous fits used to generate the concentration profiles. In the insert caption D-LEA refers to D-AavLEA1.

Figure 9: Schematic illustrating the hypothesis that LEA proteins protect CS from denaturation at interfaces by preferential adsorption. In the absence of LEA protein, CS forms aggregates at the interface. When LEA protein is present, LEA protein preferentially adsorbs to the interface and excludes the CS to the bulk. Cartoon representations of native and denatured CS were generated using Swiss-Pdb Viewer (53) based on the PDB structure 3ENJ.(54)

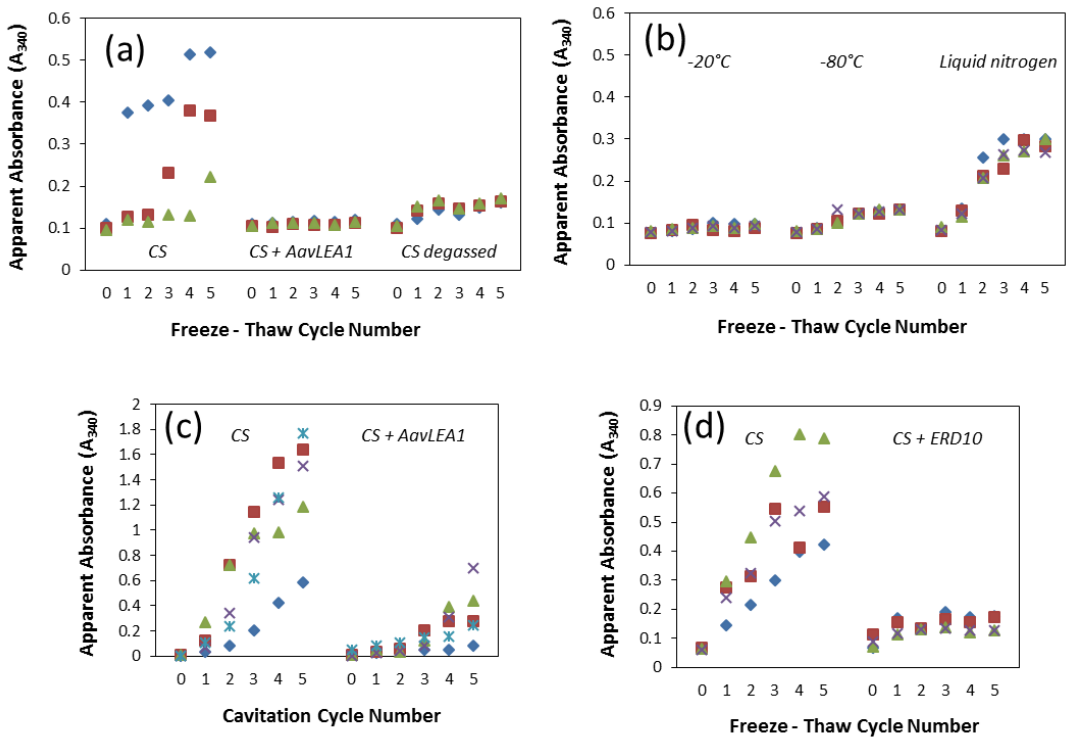

Figure 1: LEA proteins prevent CS aggregation caused by exposure to gas-liquid interfaces. Apparent absorbance at 340 nm of aqueous solutions of (a) CS, CS + AavLEA1, and degassed CS after multiple freeze-thaw cycles; (b) CS after multiple cycles of freeze-thaw at -20°C, -80°C and in liquid nitrogen; (c) CS in the absence and presence of AavLEA1 after multiple cycles of sonication; and (d) CS in the absence and presence of ERD10 after multiple freeze-thaw cycles. Concentrations of CS, AavLEA1 and ERD10 were 0.25 mg/mL. Individual data points for each replicate are shown.

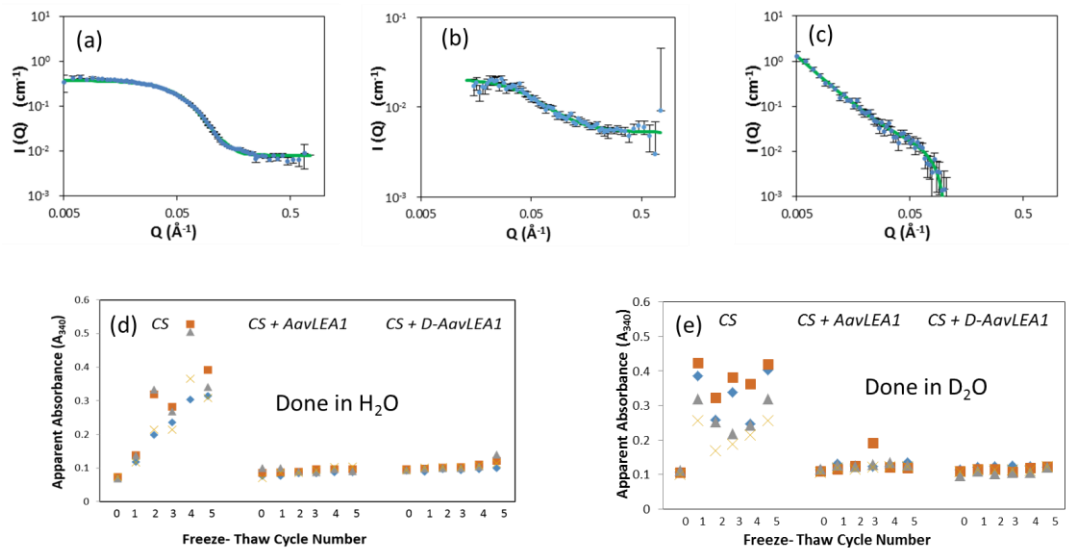

Figure 2: Characterisation of hydrogenated and deuterated AavLEA1 and CS protein. (a) The SANS pattern from 2.5 mg/ml H-CS in D_2O fits an oblate ellipsoid model with two dimensions 18.0 and 45.1 Å (b) The SANS pattern from 2.5 mg/ml H-AavLEA1 in D_2O fits well to a Gaussian coil with radius of gyration 33 Å. The low Q points were removed because of over subtraction of background. (c) The SANS pattern from 2.5 mg/ml D-AavLEA1 in 42% D_2O fits well to a correlation length model with a correlation length of 13 Å. The error bars in the SANS data correspond to the standard deviation in the neutron flux intensity. (d) Freeze-thaw cycle assays for CS and CS + H-AavLEA1 and CS+ D-AavLEA1 in H_2O. (e) Freeze-thaw cycle assays for CS and CS + H-AavLEA1and CS+ D-AavLEA1 in D_2O.

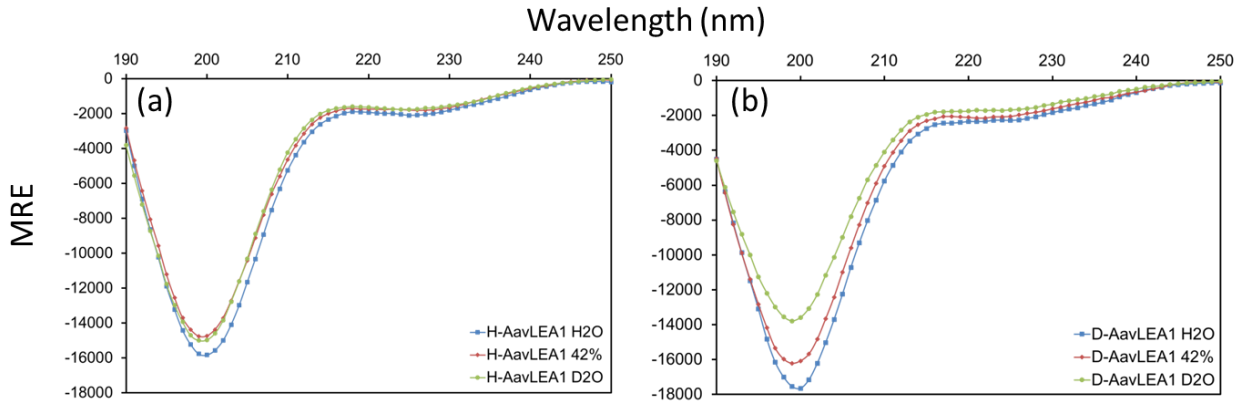

Figure 3: H-AavLEA1 and D-AavLEA1 are both disordered in solution. Far-UV CD spectra of (a) H-AavLEA1 and (b) D-AavLEA1 in H_2O, 42% D_2O and D_2O Data are displayed as mean residue ellipticities (MRE) to normalise for differences in concentration.

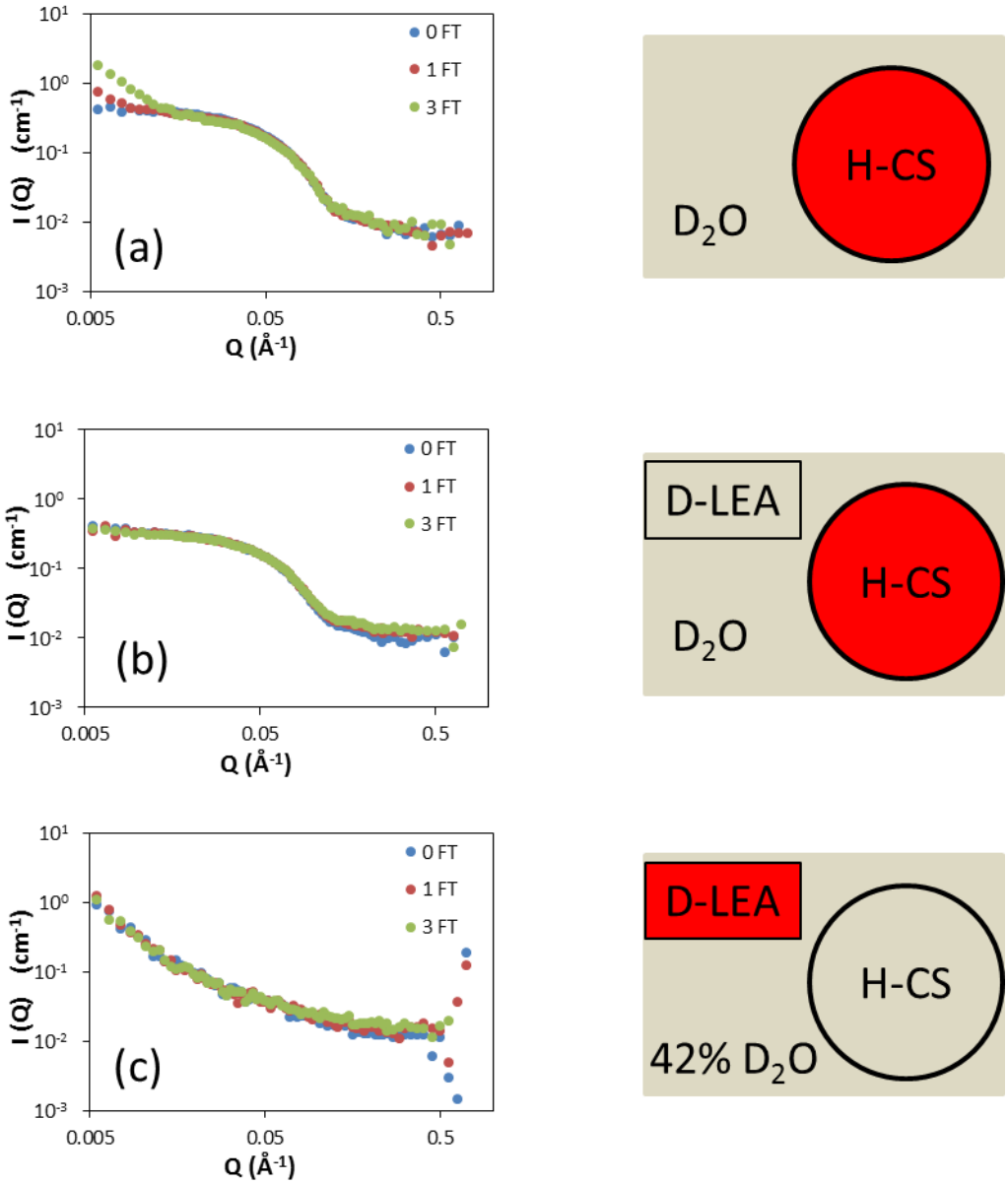

Figure 4: SANS patterns from mixtures of CS and deuterated AavLEA1 after up to three cycles of freeze-thaw. (a) 2.5 mg/ml H-CS in D_2O after zero, one and three cycles of freeze thaw. (b) 2.5 mg/mL H-CS + 2.5 mg/mL D-AavLEA1 mixture in D_2O, after zero, one and three cycles of freeze-thaw. Scattering is only observed from H-CS, and (c) 2.5 mg/mL H-CS + 2.5 mg/mL D-AavLEA1 mixture in 42% D_2O, after zero, one cycle and three cycles of freeze-thaw. Scattering is only observed from D-AavLEA1.

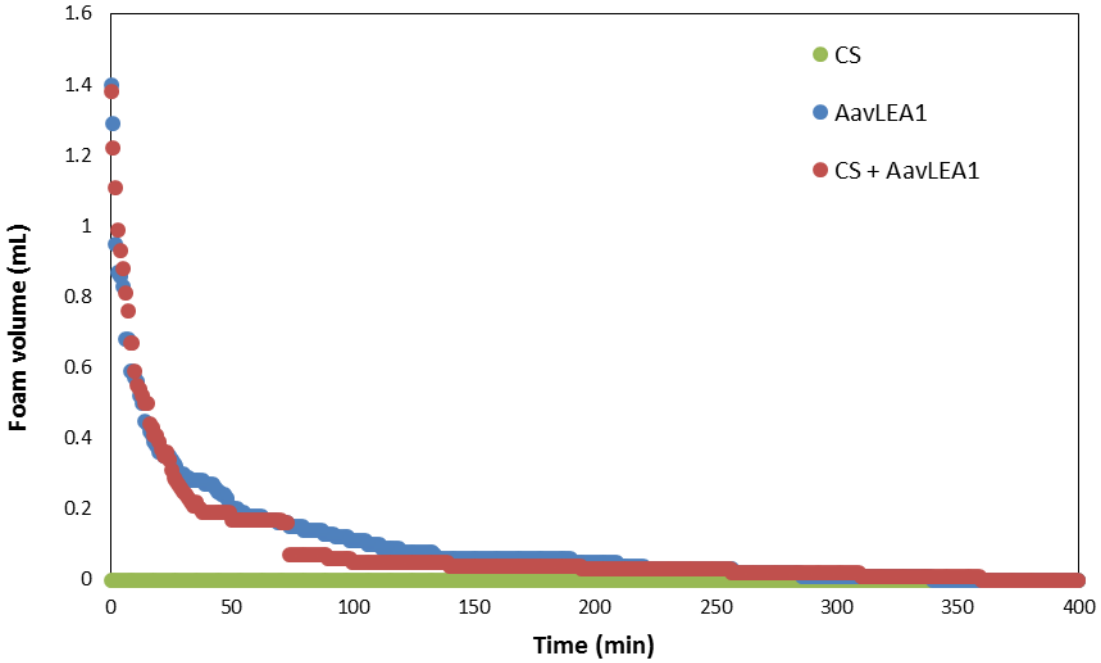

Figure 5: Foam collapse profile of 0.25 mg/mL CS, 0.25 mg/mL AavLEA1 and 0.25 mg/mL CS + 0.25 mg/mL AavLEA1 solutions. Closed 10 mL cylinders with 1 mL of each protein solution were vigorously shaken by hand 10 times, once per second, over 10 s and the foam volume was measured at various time points over 6.5 h.

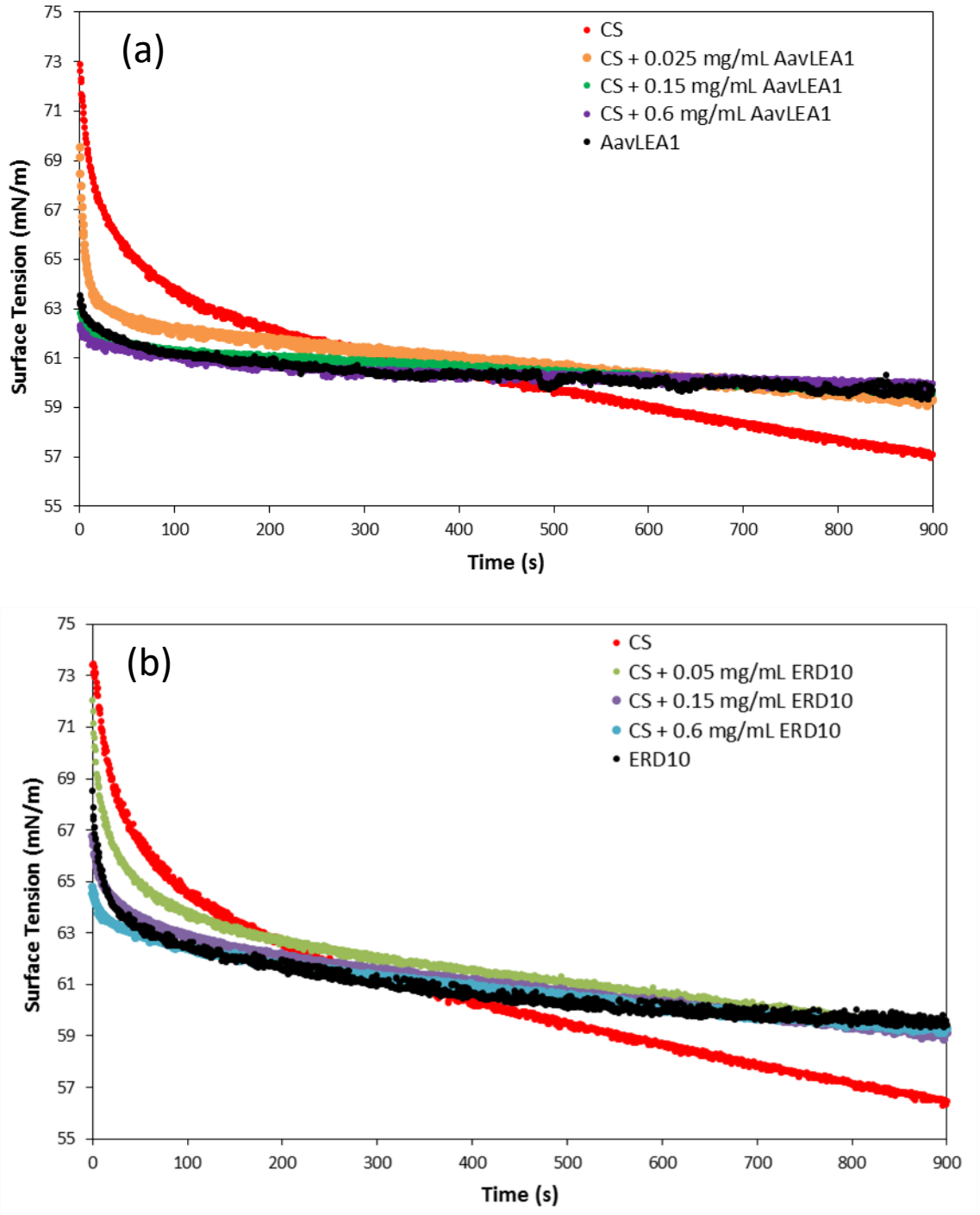

Figure 6: Dynamic surface tension profiles of 0.6 mg/mL CS, and 0.6 mg/mL CS with various concentrations of LEA proteins (a) AavLEA1 and (b) ERD10. The surface tension of each solution was monitored over 15 min using the pendant drop method. Time = 0 s denotes the start of measurement at approximately 8 s after the start of drop formation.

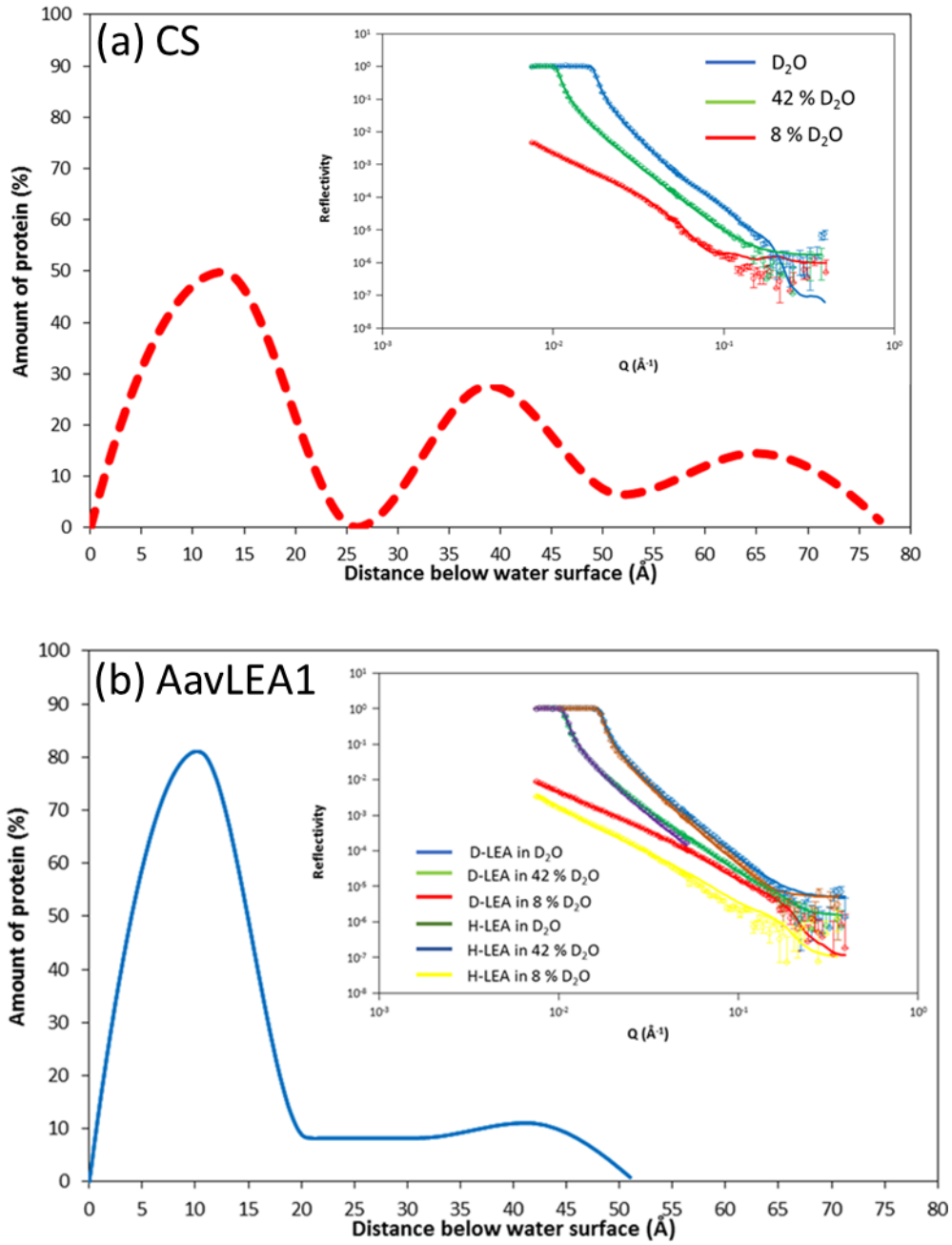

Figure 7: Neutron reflectivity profiles for 0.6 mg/ml AavLEA1 protein in water and the resulting depth profile of protein concentration from simultaneous fitting of all reflectivity profiles. (a) 0.6 mg/ml CS in various water contrasts. (b) H- and D-AavLEA1 protein in different water contrasts. The contribution from AavLEA1 is denoted in the blue solid lines, and the CS contribution is shown by the red dotted lines. Inserts to figures show the reflectivity profiles in the various contrasts and the simultaneous fits used to generate the concentration profiles. In the insert caption D-LEA refers to D-AavLEA1.

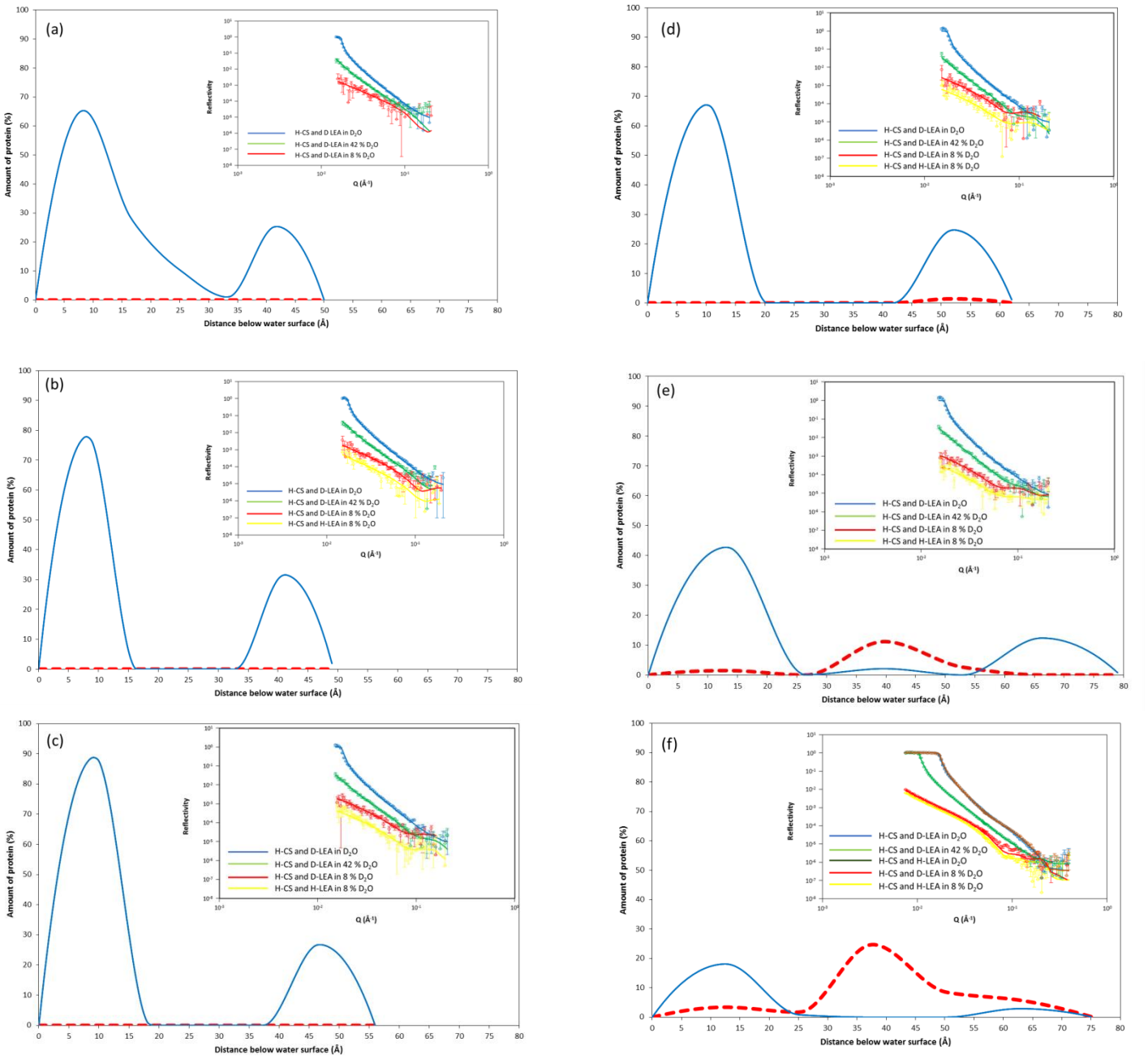

Figure 8: Protein concentration profiles as measured by neutron reflection at the air-water interface for 0.6 mg/mL CS + 0.6 mg/mL AavLEA1 in water at various times. (a) 30 s, (b) 1 min, (c) 5 min, (d) 30 min, (e) 60 min, (f) 2 h. The contribution from AavLEA1 is denoted in the blue solid lines, and the CS contribution is shown by the red dotted lines. Inserts to figures show the reflectivity profiles in the various contrasts and the simultaneous fits used to generate the concentration profiles. In the insert caption D-LEA refers to D-AavLEA1.

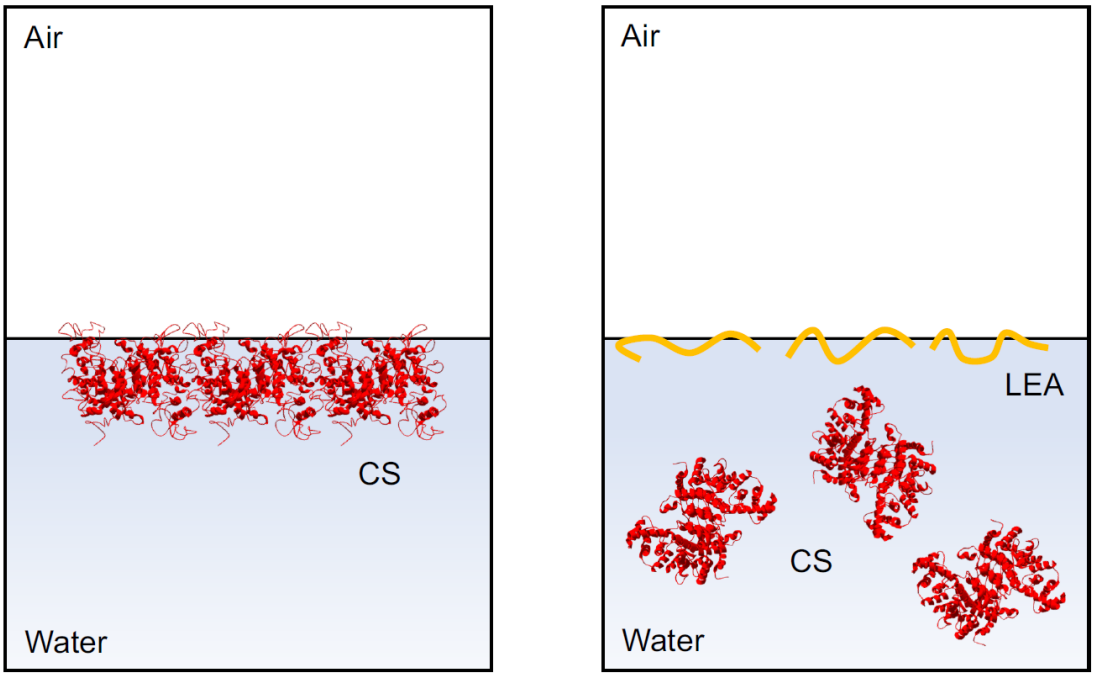

Figure 9: Schematic illustrating the hypothesis that LEA proteins protect CS from denaturation at interfaces by preferential adsorption. In the absence of LEA protein, CS forms aggregates at the interface. When LEA protein is present, LEA protein preferentially adsorbs to the interface and excludes the CS to the bulk. Cartoon representations of native and denatured CS were generated using Swiss-Pdb Viewer (53) based on the PDB structure 3ENJ.(54)